Accepted Manuscript

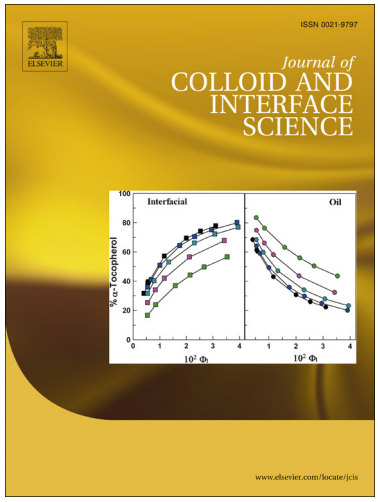

Modulating *in vitro* Release and Solubility of Griseofulvin Using Functionalised Mesoporous Silica Nanoparticles

Siddharth Jambhrunkar, Zhi Qu, Amirali Popat, Surajit Karmakar, Chun Xu, Chengzhong Yu

PII: S0021-9797(14)00576-1
DOI: http://dx.doi.org/10.1016/j.jcis.2014.08.019
Reference: YJCIS 19754

To appear in: *Journal of Colloid and Interface Science*

Received Date: 25 May 2014
Accepted Date: 9 August 2014

Please cite this article as: S. Jambhrunkar, Z. Qu, A. Popat, S. Karmakar, C. Xu, C. Yu, Modulating *in vitro* Release and Solubility of Griseofulvin Using Functionalised Mesoporous Silica Nanoparticles, *Journal of Colloid and Interface Science* (2014), doi: http://dx.doi.org/10.1016/j.jcis.2014.08.019

Modulating *in vitro* Release and Solubility of Griseofulvin Using Functionalised Mesoporous Silica Nanoparticles

Siddharth Jambhrunkar[a], Zhi Qu[a], Amirali Popat[b,c], Surajit Karmakar[a], Chun Xu[a], Chengzhong Yu[a]*

[a]Australian Institute for Bioengineering and Nanotechnology, The University of Queensland, Brisbane, QLD 4072, Australia.

[b]The School of Pharmacy, The University of Queensland, Brisbane, QLD 4072, Australia.

[c]Mucosal Diseases Group, Mater Research Institute – The University of Queensland, Translational Research Institute, 37 Kent St, Woolloongabba, QLD 4102.

* Corresponding author. Fax: +61 7 3346 3973; Tel: +61 7 3346 3283. E-mail: c.yu@uq.edu.au

Abstract:

Mesoporous silica nanoparticles (MCM-41) were used as a carrier system to study the influence of surface charge and hydrophobicity on solubility and *in-vitro* drug release behavior of Griseofulvin, a potent antifungal drug with low water solubility. Bare MCM-41 with a pure silica composition, MCM-41 after amino functionalization (MCM-41-NH_2) and methyl functionalization (MCM-41-CH_3) were used in this study followed by encapsulation of griseofulvin. Various characterization techniques have been employed to confirm the successful drug loading inside the nanopores. The surface functionalization on MCM-41 is found to have significant effect on griseofulvin's *in vitro* release and solubility. Both negatively and positively charged surface showed enhancement in solubility and drug release of griseofulvin. However, the hydrophobic modification led to a retarded drug release, which is caused by the poor wetting effect in the case of MCM-41-CH_3 nanoparticles.

Keywords: mesoporous silica, surface charge, hydrophobicity, griseofulvin, drug release, solubility

1. Introduction

Relatively higher proportions of newly emerging drug molecules from high throughput screening are hydrophobic (poor aqueous solubility), posing a major obstacle in clinical applications.[1,2] Solubility enhancement is traditionally achieved by various processes such as

salt formation, co-solvents, complexation, and solid dispersion to name a few. These techniques, however, suffer from uncontrolled precipitation, solvent toxicity and stability concerns.[3-6] The main emphasis for solubility enhancement till date in the pharmaceutical fraternity relies on particle size reduction, as reflected by Ostwald-Freundlich equation.[7] Particle size reduction techniques such as comminution, micronization and spray drying are conceived to be efficient, reproducible and economically viable. However, this process leads to induction of physical stress on drug particles, tendency to agglomerate on standing and is inapt for thermolabile drugs. The development of effective carrier systems provides another pathway to enhance the drug solubility as well as to control the release profile. Several delivery systems such as surfactant complexes, liposomes, hydrogels, and polymeric nanoparticles have been developed but suffer from synthesis complexity and poor biological stability.[8-10]

Mesoporous silica nanoparticles (MSNs) such as MCM-41[11] and SBA-15[12], with unique features of ordered structure, high surface area, large pore volume, tuneable pore size, ease of surface functionalization[13] and biocompatibility have attracted increased attention in drug delivery field since the last decade.[14] The influence of pore size of MSNs has been studied for drug, peptide, protein and enzyme immobilization. [15-18] MSNs provide an adjustable pore size at nanoscale for the confinement of drug molecules and hence the size of drug particles can be reduced at nanoscale leading to solubility enhancement.[19-21] MSNs surface functionalisation also plays an important role in drug encapsulation and release.[22,23] Surface functionalized MSNs with 3-aminopropyl triethoxysilane help in achieving high drug loading and slower drug release.[13,22,24] MSNs modified by 2-cyanopropyltriethoxysilane and mercaptopropyltrimethoxysilane improved drug efficacy by achieving high cell specificity when tested in cell lines.[25,26] MSNs were modified to obtain hydrophobic surface using 1, 1, 1, 3, 3, 3-hexamethyldisilazane, and ibuprofen release test showed that the drug release was inversely proportional to the degree of hydrophobicity.[27] Despite numerous studies highlighting the significance and advantage of MSNs for enhancing drug solubility and the effect of surface functionalization of MSNs on drug release, there is no study to compare the influence of surface charge and hydrophobicity on both drug solubility and drug release.

Griseofulvin (GRIS), a potent antifungal drug, belongs to BCS class II and is slightly soluble in water.[28] Several studies have been reported addressing the solubility and/or dissolution enhancement of griseofulvin using processes such as solid dispersions[19,29], complexation with cyclodextrin[30], microemulsions[31] and deformable membrane vesicles.[28] In a recent study, an inclusion complex of griseofulvin – β-cyclodextrin was formed and grafted on the silica surface to study the adsorption kinetics, confirming the successful encapsulation of griseofulvin in β-cyclodextrin. [32] However, the drug release or solubility behavior was not reported. To date the encapsulation of GRIS inside MSNs has not been reported.

In this study, we report the influence of surface charge and hydrophobicity of MSNs on solubility and drug release behavior of griseofulvin in a series of MCM-41 materials (Fig.1), including bare MCM-41, amino functionalised MCM-41 (MCM-41-NH_2) and methyl functionalized MCM-41 (MCM-41-CH_3). The surface modified MSNs were synthesized to obtain similar pore size to avoid the influence of pore size in further evaluations. Griseofulvin was encapsulated in the pore channels of MSNs by a simple rotavap technique. We studied the influence of surface chemistry on drug solubility and drug release by comparing negatively and positively charged MCM-41 with hydrophobic MCM-41-CH_3. To the best of our knowledge this is the first report to study the influence of surface modification of MSNs on griseofulvin's *in vitro* release and solubility.

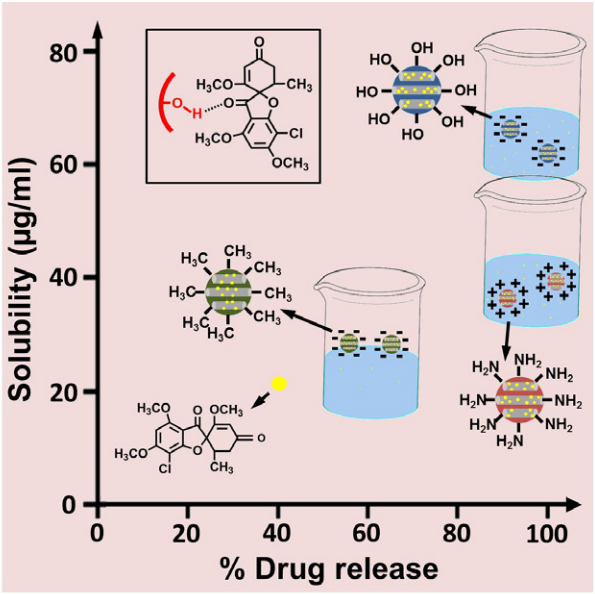

Fig 1. A schematic representation comparing the solubility and *in vitro* drug release of griseofulvin from MCM-41-GRIS, MCM-41-NH_2-GRIS and MCM-41-CH_3-GRIS samples. Inset represents the binding of griseofulvin to the interior pore wall of MCM-41, MCM-41-NH_2 and MCM-41-CH_3 samples. Free drug is represented in yellow color. Inset shows the binding of GRIS in MCM-41.

2. Experimental

2.1. Materials

Cetyl trimethylammonium bromide (CTAB), tetraethoxy orthosilicate (TEOS), (3-aminopropyl)triethoxysilane (APTES), chlorotrimethylsilane (TMCS), sodium lauryl sulphate (SLS) and griseofulvin (GRIS) were purchased from Sigma-Aldrich. Reagent grade sodium hydroxide (NaOH) was received from ChemSupply. Methanol AR and Toluene were purchased from RCI labscan and Merck, respectively.

2.2. Characterization

X-ray diffractograms (XRD) and wide angle XRD (WXRD) were recorded on a Rigaku Miniflex X-ray diffractometer with Fe-filtered Co radiation (λ = 1.79 Å). Transmission electron microscopy (TEM) images were obtained with a JEOL 1010 microscope operated at 100 kV. Scanning electron microscopy (SEM) characterization was performed using Hitachi SU3500 operated at 5 kV and working distance of 5.5 cm. Nitrogen physisorption measurements were carried out at -196 °C by using a Micromeritics Tristar II 3020 system. MCM-41, MCM-41-NH_2 and MCM-41-CH_3 samples were degassed at 100 ℃ whereas griseofulvin encapsulated MCM-41 (MCM-41-GRIS), MCM-41-NH_2 (MCM-41-NH_2-GRIS) and MCM-41-CH_3 (MCM-41-CH_3-GRIS) samples were degassed at 50 ℃ overnight on a vacuum line. The pore-size distribution was measured from the adsorption branch of the isotherm using BJH model. Fourier transform infrared (FTIR) spectra were recorded on ThermoNicolet Nexus 6700 FTIR spectrometer equipped with Diamond ATR (attenuated total reflection) Crystal. For each spectrum, 128 scans and 4 cm^{-1} resolution was applied over the range of 400–4000 cm^{-1}. Particle size and zeta potential was measured on a Malvern Zetasizer Nano-ZS. The thermogravimetric analysis (TGA) was performed by a Setaram TG92 instrument with a heating rate of 5 ℃/min in air flow. Griseofulvin concentration was determined using UV-VIS spectrophometer (Shimadzu UV-2450).

2.3. Synthesis of MCM-41

MCM-41 synthesis was performed with slight modification to a previously reported method by Yang et al.[33] Briefly, 1.0 g of CTAB was dissolved in 480 g of deionized water under stirring at room temperature followed by addition of 3.5 mL of NaOH (2 M) and increasing the temperature to 80 °C. Then, 6.7 mL of TEOS was added into the mixture as a silica source at 80 °C under continuous stirring for an additional 2 h. The resultant product was collected by filtration and dried at room temperature. The as-synthesized MCM-41 was divided into three parts. One-third of the material was subjected to solvent extraction process for the removal of surfactant template and labelled as MCM-41. Another one-third of the material was solvent extracted and used for the preparation of methyl modified MCM-41. The remaining as-synthesized material was utilized for the synthesis of amino modified MCM-41.

Surfactant template was removed by a reported method by Lu *et. al.*[34] with some modification. 0.3 g of as-synthesized material was added to 32 mL of methanol under stirring and the temperature was increased to 60 °C. To this suspension, 2.0 mL of conc. HCl was added and kept under continuous stirring for 36 h. Later the suspension was centrifuged and washed with methanol twice to ensure complete surfactant removal. The final product was dried at 50 °C overnight to be used for further studies.

2.4. Synthesis of amino modified MCM-41-NH_2

Amino modification was performed according to a published report with slight changes.[35] Typically, 0.4 g of as-synthesized MCM-41 was added to 25 mL of methanol under stirring at RT followed by the addition of 1.5 mL of APTES. The suspension was stirred overnight at RT. The amino functionalized MCM-41 with surfactant template still present in it was then retrieved by centrifugation and washed with methanol twice. The material was then dried at 50 °C overnight before subjected to solvent extraction process for surfactant template removal as described earlier.

2.5. Synthesis of methyl modified MCM-41

Methyl modification was performed according to a published report.[36] Generally, 0.4 g of MCM-41 after solvent extraction was added to 20 mL of TMCS solution in toluene with a concentration of 5 wt% under stirring at 70 °C. The suspension was stirred for additional 24 h at 70 °C. The methyl functionalized MCM-41 was then centrifuged and washed with toluene and ethanol. The material was then dried at 50 °C overnight for further studies.

2.6. Griseofulvin loading and in vitro release measurements

Griseofulvin loading was performed using rotary evaporation technique. 160 mg of MCM-41 was placed in a rotary evaporation flask and 40 mg of griseofulvin was added to it followed by the addition of 10 ml of dichloromethane to achieve 20% w/w drug loading theoretically. This mixture was sonicated for 2 minutes and the solvent was slowly evaporated using rotary evaporator at 50 ℃ with circulating water temperature maintained at 5 ℃ to obtain griseofulvin loaded MCM-41. Evaporation process was continued till all the solvent is removed and dried powder could be observed in the flask. Dried griseofulvin loaded MCM-41 sample (MCM-41-GRIS) was collected from the flask and used for further studies. Similar procedure was followed for MCM-41-NH_2 and MCM-41-CH_3 materials. Dried griseofulvin loaded MCM-41-NH_2 and MCM-41-CH_3 materials are denoted as MCM-41-NH_2-GRIS and MCM-41-CH_3-GRIS, respectively.

2.6. *In vitro* release and solubility studies

The *in vitro* release of griseofulvin from MCM-41-GRIS, MCM-41-NH_2-GRIS and MCM-41-CH_3-GRIS was evaluated using dialysis bag technique.[18,37,38] MCM-41-GRIS, MCM-41-NH_2-GRIS and MCM-41-CH_3-GRIS equivalent to 1 mg of griseofulvin was weighed and suspended in 1 mL of 0.5% SLS. This suspension was then placed in dialysis bag with 10 kDa molecular weight cutoff and was immersed into 9 mL of 0.5% SLS at 37 °C with continuous stirring. At pre-determined time intervals, 1 mL of the samples were withdrawn and immediately replaced with

an equal volume of dissolution medium to maintain the sink condition. The samples withdrawn at pre-determined time intervals were then properly diluted and analyzed for griseofulvin content using UV-VIS spectrophotometer at 296 nm.

Griseofulvin solubility studies were conducted by adding an excessive quantity of griseofulvin and MCM-41-GRIS, MCM-41-NH_2-GRIS and MCM-41-CH_3-GRIS material to 2 mL of water. The mixture was kept for shaking for 48 h at 37 ℃. The suspension was then centrifuged and the supernatant was analyzed for griseofulvin content using a UV-VIS spectrophotometer at 296 nm.

3. Results and discussion

3.1. Material characterization

The XRD patterns of MCM-41 material (Fig. 2A) show three well resolved diffraction peaks at 2θ of 2.44, 4.27 and 4.93° with a reciprocal d-spacing ratio close to 1: √3: 2, which can be indexed as 100, 110 and 200 reflections of an ordered two dimensional (2D) hexagonal mesostructure with a pore symmetry of *p6mm*. The positions of three diffraction peaks for MCM-41-NH_2 and MCM-41-CH_3 are similar to that of MCM-41 demonstrating retention of ordered structure after surface functionalization. After encapsulation of griseofulvin in MCM-41, MCM-41-NH_2 and MCM-41-CH_3, no shift was observed for the three diffraction peaks, indicating the drug loading process does not alter the ordered mesostructure.

To study the nature of griseofulvin encapsulated in MCM-41 materials, WXRD study was performed. The WXRD patterns (Fig. 2B) were obtained for MCM-41 materials with and without griseofulvin loading along with the physical mixtures of griseofulvin and respective MCM-41 materials. Pure griseofulvin is a crystalline compound showing sharp diffractions in the 2θ range of 10-40°. The amorphous nature of MCM-41, MCM-41-NH_2 and MCM-41-CH_3 material is evidenced from the broad peak in the 2θ range of 20-30°.[39,40] The physical mixture of three MCM-41 materials and griseofulvin (MCM-41-GRIS PM, MCM-41-NH_2-GRIS PM and MCM-41-CH_3-GRIS PM) show diffraction peaks corresponding to pure griseofulvin. However, for MCM-41-GRIS, MCM-41-NH_2-GRIS and MCM-41-CH_3-GRIS using the rotavap technique to encapsulate griseofulvin, no obvious diffraction peaks originating from GRIS can be observed, suggesting that GRIS is entrapped inside the nanopores with an amorphous nature.[39,40]

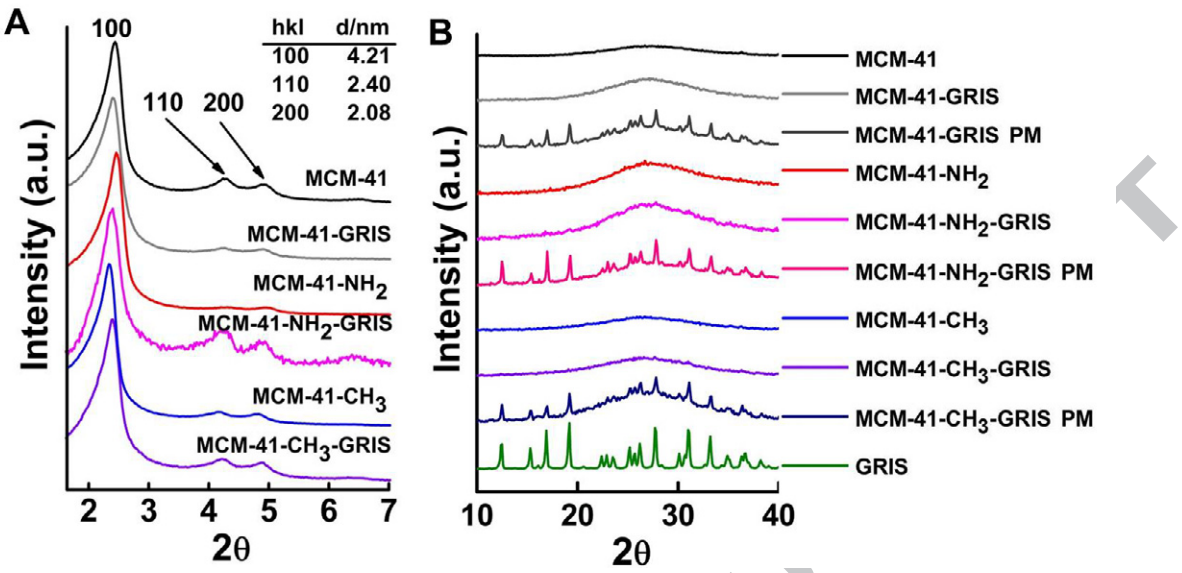

Fig 2. (A) XRD patterns of MCM-41 materials with and without griseofulvin loading. (B) WXRD patterns of MCM-41 materials with and without griseofulvin loading and physical mixtures of griseofulvin with unfunctionalized and functionalized MCM-41 materials.

Typical TEM images of MCM-41, MCM-41-NH_2 and MCM-41-CH_3 are shown in Fig. 3. Because three materials were prepared from the same mother solution, they show similar morphologies as nanoparticles with 100-200 nm in sizes. For each particle shown in Figs. 3a-c, parallel channel-like or hexagonally arrayed porous structures can be seen, in accordance with a hexagonal mesostructure. The TEM results also suggest that surface functionalization of MCM-41 in our experiments did not affect the hexagonal structure, consistent with the XRD characterisations. Dynamic light scattering (DLS) measurements (Fig. 3d) reveal a mean size of 190 nm for all the MSN materials – MCM-41 (PDI = 0.182), MCM-41-NH_2 (PDI = 0.165) and MCM-41-CH_3 (PDI = 0.223, similar to the TEM results.

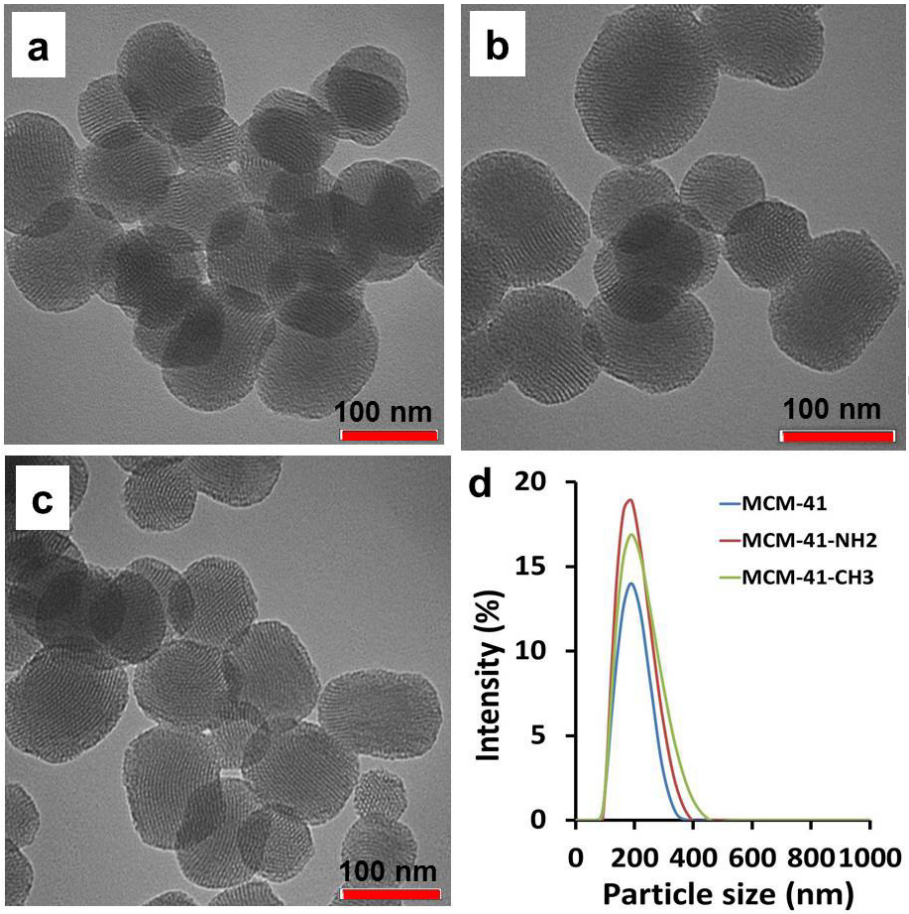

Fig 3. Transmission Electron Microscopy (TEM) image of MCM-41(a), MCM-41-NH_2 (b) and MCM-41-CH_3 (c) materials. DLS size measurements of MCM-41, MCM-41-NH_2 and MCM-41-CH_3 materials (d).

The nitrogen adsorption/ desorption isotherms of MCM-41, MCM-41-NH_2 and MCM-41-CH_3 exhibit a typical type IV isotherm with a steep capillary condensation step at a relative pressure (P/P_0) range of 0.2-0.4 (Fig. 4A), characteristic of MCM-41 type mesoporous materials. From the pore size distribution curves (Fig. 4B), it is shown that MCM-41 material has a pore size of 2.57 nm. MCM-41-NH_2 has a pore size of 1.99 nm, suggesting that a small amount of the silica source (APTES) can replace the surfactants during the post-modification process starting from the as-synthesized MCM-41.[35] If the post-modification of amino groups starts from MCM-41 after removing the surfactants, the pores will be blocked (data not shown).[41] MCM-41-CH_3 exhibits a pore size centered at 2.13 nm, suggesting slight decrease in the pore size due to the presence of small amount of methyl groups in pore channels during the modification process. Our observation is consistent with previous reports on the hydrophobic modification of mesoporous materials after removing the surfactants, where the pore size is reduced by 0.25 – 0.65 nm. [36,42]

After griseofulvin encapsulation in MCM-41, MCM-41-NH_2 and MCM-41-CH_3 materials, the pore size of MCM-41-GRIS, MCM-41-NH_2-GRIS and MCM-41-CH_3-GRIS have been decreased

to 1.87, 1.68, and 2.02 nm, respectively. The drug encapsulation also results in decrease in surface area and pore volume. For example, the surface area and surface volume for MCM-41-GRIS decreases to 562 m^2/g and 0.45 cm^3/g compared to MCM-41 from 900 m^2/g and 0.86 cm^3/g respectively. Similar trend was observed for MCM-41-NH_2-GRIS and MCM-41-CH_3-GRIS materials as well. All the textural parameters for MSNs are summarized in Table 1 for comparison.

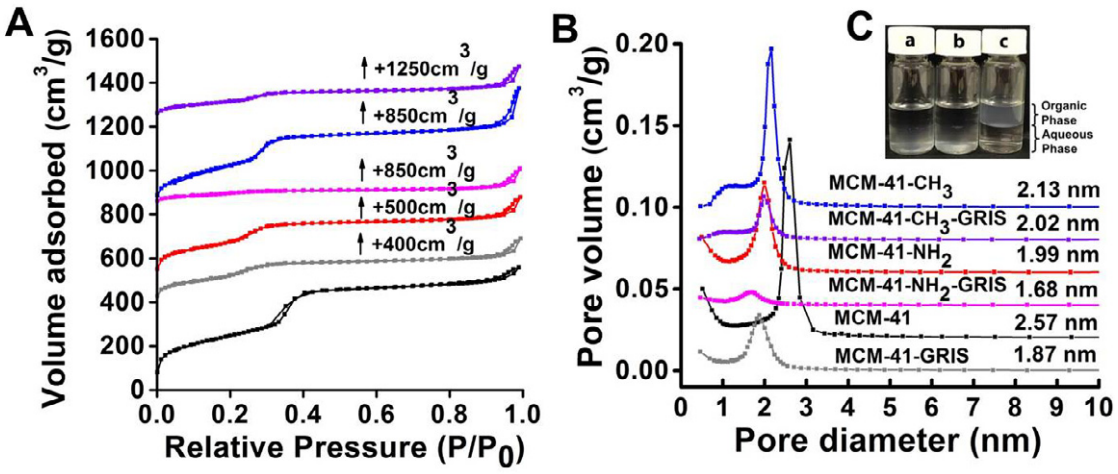

Fig 4. A) N_2 adsorption/desorption isotherms and B) BJH pore-size distribution plot for unfunctionalized and functionalized MCM-41 materials with and without griseofulvin loading. C) Digital image of a) MCM-41, b) MCM-41-NH_2 and c) MCM-41-CH_3 demonstrating the hydrophobicity of materials by dispersing them in organic (ether) – aqueous (water) composition.

The surface modification of MCM-41 materials was further analyzed by measuring zeta potential (Z.P.). As shown from Table 1, MCM-41 shows a Z.P. of -33.5 ± 0.42 mV, while MCM-41-NH_2 and MCM-41-CH_3 display Z.P. of 33.2 ± 0.20 and -12.7 ± 0.60 mV, respectively, confirming the successful surface modification of MCM-41 materials. The surface modification is also evidenced by dispersing the materials in ether – water composition as shown in Fig. 4C. Both MCM-41 and MCM-41-NH_2 materials were totally dispersed in aqueous phase with a hazy appearance, showing a hydrophilic nature. On the other hand, MCM-41-CH_3 material was completely dispersed in organic phase displaying its hydrophobic nature.

Table 1. Physicochemical properties of unfunctionalized and functionalized MCM-41 materials with and without griseofulvin loading.

Sample	*a* (nm)	*P* (nm)	S_{BET} (m^2/g)	V_p (cm^3/g)	*Z.P.*(mV)

MCM-41	4.86	2.57	900	0.86	-33.5 ± 0.42
MCM-41-NH_2	4.82	1.99	785	0.68	33.2 ± 0.20
MCM-41-CH_3	5.07	2.13	904	0.81	-12.7 ± 0.60
MCM-41-GRIS	4.94	1.87	562	0.45	-34.2 ± 0.34
MCM-41-NH_2-GRIS	4.95	1.68	179	0.24	34.5 ± 0.62
MCM-41-CH_3-GRIS	4.95	2.02	328	0.35	-12.4 ± 1.30

Note: *a*=cell dimension; S_{BET} = BET surface area; V_p = pore volume; *P* = pore size; Z.P. = Zeta potential.

3.2. Adsorption of griseofulvin

The modification of MCM-41 materials with amino and methyl groups as well as the encapsulation of griseofulvin in MCM-41 materials was confirmed by FTIR analysis as shown in Fig. 5. Bare MCM-41 material exhibits two peaks at 803 and 1060 cm^{-1} (Figure 5C), which can be indexed to symmetric and asymmetric Si–O–Si stretching (ν_s(Si-O-Si) and ν_a(Si-O-Si)), respectively. Two bands with low intensity are observed at 3740 cm^{-1} and 1630 cm^{-1} which can be indexed to the isolated silanol (ν(O-H)) and bending mode of physiosorbed water respectively (Figs. 5A and 5B).[21,44] The silanol peak disappeared when amino and methyl modifications are performed on MCM-41. The amino modification resulted in appearance of peaks at 2929, 1626 and 1518 cm^{-1} which can be attributed to C–H stretching, N–H bending and N–H stretching vibrations of aminopropyl group anchored on the surface of MCM-41.[13,45,46] The methyl modification results in the peak at 2962 cm^{-1} which can be attributed to C–H vibration and band of peaks at 1255, 848 and 758 cm^{-1} attributed to Si-CH_3 of methyl group from TMCS.[42,47] Pure griseofulvin displays two distinct peaks at 1704 and 1658 cm^{-1} which is attributed to the stretching of carbonyl group of benzofuran and cyclohexenone respectively present in its structure.[19,29] The peak at 1704 cm^{-1} appears as broadened peak in MCM-41-GRIS. Similarly the peak at 1658 cm^{-1} peak was broadened and shifted to 1649 cm^{-1} in MCM-41-GRIS. The broadening of these two peaks can be attributed to the hydrogen bonding between isolated silanols located in the interior surface of MCM-41 and carbonyl group of benzofuran and cyclohexenone of griseofulvin.[19,29] Moreover, peaks in the range of 1617-890 cm^{-1} in griseofulvin can also be seen in MCM-41-GRIS indicating the encapsulation of griseofulvin. Similar results were observed for MCM-41-NH_2-GRIS and MCM-41-CH_3-GRIS samples confirming the successful adosrption of griseofulvin.

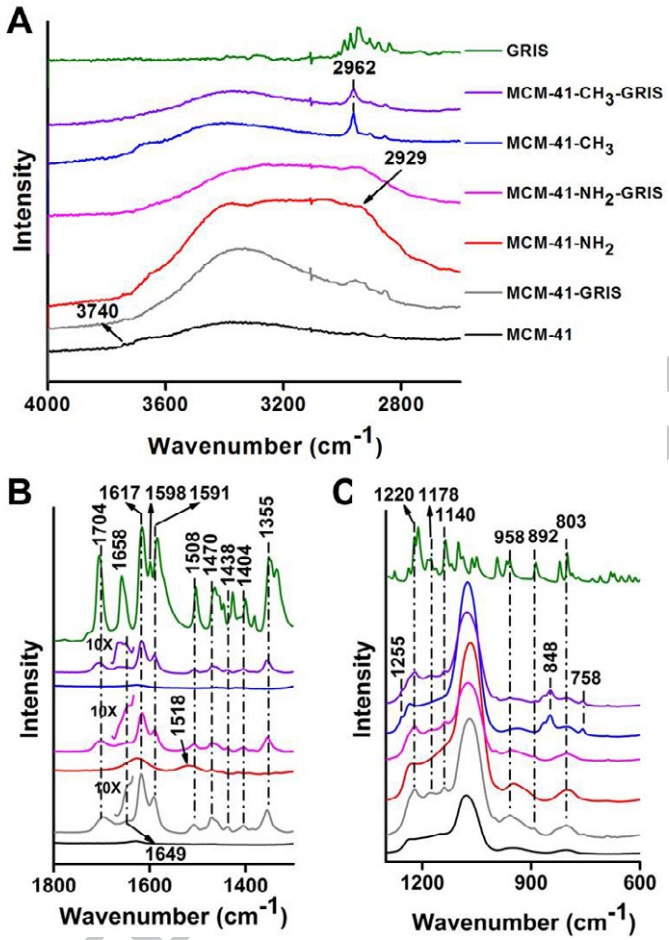

Fig 5. FTIR spectra of unfunctionalized and functionalized MCM-41 materials with and without griseofulvin loading.

TGA analysis was used to evaluate the griseofulvin loading amount in different samples under study (Fig. 6A). Griseofulvin encapsulated in MCM-41, MCM-41-NH_2 and MCM-41-CH_3 materials by rotary evaporation technique was found to be 19.92 %, 15.76 % and 19.90% respectively, indicating a high loading efficiency (80-95%) of the process, in accordance with previous reports.[21,48] For comparison, physical mixtures of griseofulvin and MCM-41 (MCM-41-GRIS PM), MCM-41-NH_2 (MCM-41-NH_2-GRIS PM) and MCM-41-CH_3 (MCM-41-CH_3-GRIS PM) materials were prepared. MCM-41-GRIS PM, MCM-41-NH_2-GRIS PM and MCM-41-CH_3-GRIS PM samples showed weight loss of 19.89%, 20.16% and 21.05% respectively (Fig. 7A). The hydrophobic modification inhibits the aqueous wetting of MCM-41-CH_3 by methyl groups present on the material which is evident by the % wt. loss at 100℃ as seen from Fig. 6A and 7A. The moisture loss for MCM-41 and MCM-41-NH_2 is 7 and 11 % whereas 3% for MCM-41-CH_3 material thus demonstrating the effect of hydrophobicity on moisture uptake.

Differential scanning calorimetry (DSC) analysis was performed to further confirm the crystallinity of griseofulvin in MCM-41-GRIS, MCM-41-NH_2-GRIS and MCM-41-CH_3-GRIS

materials (Fig. 6B). Pure griseofulvin clearly displays a sharp melting point peak at 220 ℃. A weak signal can be observed for MCM-41-GRIS PM, MCM-41-NH_2-GRIS PM and MCM-41-CH_3-GRIS PM samples indicating the existence of griseofulvin's crytalline state in their respective physical mixtures (Fig. 7B). However, this peak cannot be seen in MCM-41-GRIS, MCM-41-NH_2-GRIS and MCM-41-CH_3-GRIS samples (Fig. 6B), indicating griseofulvin's non-crystalline state and its succesful loading as nano-sized aggregates in the pore channels of these MCM-41 materials.[20,49]

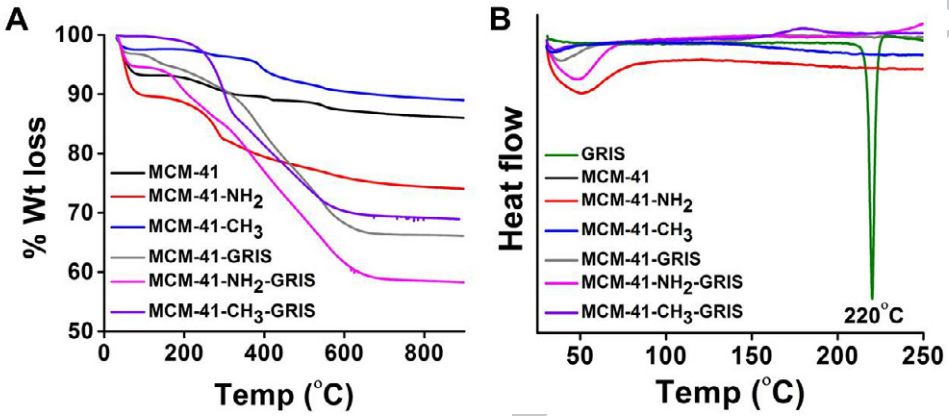

Fig 6. A)TGA curves and B) DSC curves of unfunctionalized and functionalized MCM-41 materials with and without griseofulvin loading.

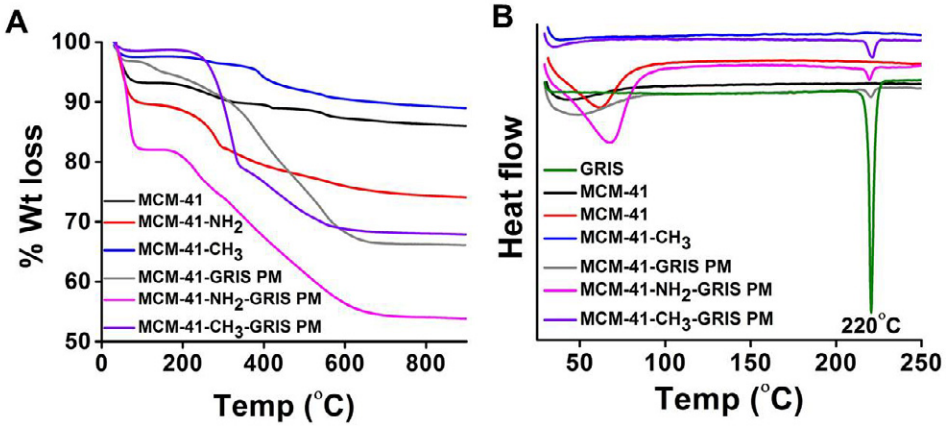

Fig 7. TGA (A) and DSC (B) curves of physical mixtures of griseofulvin with unfunctionalized and functionalized MCM-41 materials.

SEM images of GRIS, MCM-41, MCM-41-GRIS and MCM-41-GRIS PM samples were collected to provide further information on the drug loading (Fig. 8). GRIS shows a particulate morphology with irregular shapes and sizes (Fig. 8A). For MCM-41, spherical nanoparticles are observed with size of 100-200 nm (Fig. 8B), in accordance with TEM observations and previous reports.[18] In the case of MCM-41-GRIS, the morphology is similar to that of MCM-41 (Fig. 8C); no irregular shaped particles are observed.

However, both spherical MCM-41 and irregular GRIS particles are observed in MCM-41-GRIS PM (Fig. 8D). The above studies, including WXRD, FTIR, DSC and SEM characterisations, support the conclusion that GRIS is successfully encapsulated in the nanopores of MCM-41.

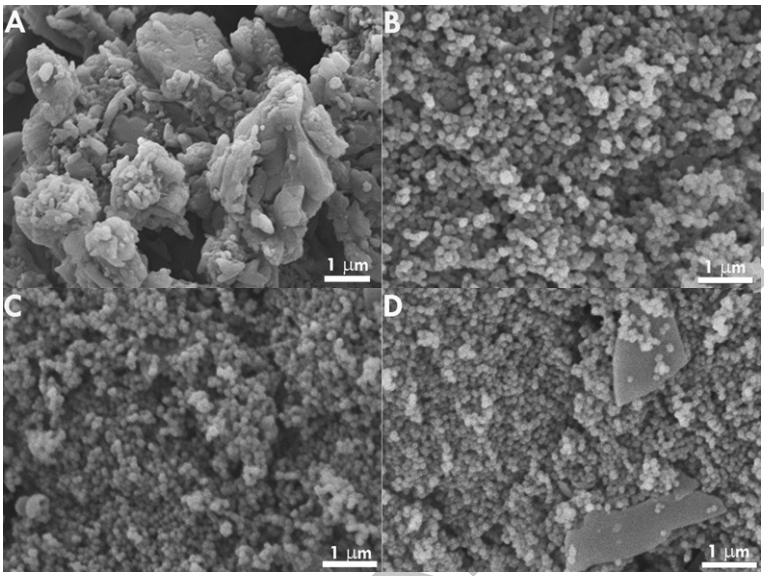

Fig. 8 SEM images of pure griseofulvin (A), MCM-41 (B), MCM-41-GRIS (C) and MCM-41-GRIS PM (D).

3.3. *In vitro* release and Solubility studies

To compare the effect of surface charge and hydrophobicity in griseofulvin encapsulated MCM-41 materials, griseofulvin release was studied in 0.5% SLS (under sink conditions) as the dissolution medium. After 1 h, the release of griseofulvin from MCM-41-GRIS, MCM-41-NH_2-GRIS and MCM-41-CH_3-GRIS was found to be 13.40, 7.60 and 2.69% respectively compared to 7.37% from pure griseofulvin (Fig. 9). Until 8 h, the griseofulvin release from MCM-41-NH_2-GRIS (26.15%) was similar to that of pure griseofulvin (26.62%) while from that of MCM-41-GRIS and MCM-41-CH_3-GRIS was 45.19% and 8.85% respectively. Griseofulvin was completely released from MCM-41-GRIS after 48 h. After 8 h, griseofulvin's release from MCM-41-NH_2-GRIS was relatively faster compared to pure griseofulvin and took 96 h for its complete release. The slower release from MCM-41-CH_3-GRIS was attributed to the hydrophobic effect derived from methyl functionlaization of TMCS on the surface.[27] At the end of 96 h, MCM-41-CH_3-GRIS released 60% of griseofulvin whereas for pure griseofulvin 88% was dissolved.

Encapsulation of griseofulvin in negatively charged MCM-41 resulted in faster release while positively charged MCM-41-NH_2 leads to relatively slower release. The faster release from MCM-41-GRIS could be attributed to the presence of griseofulvin as nano-sized aggregates in the pore channels of MCM-41.[18,49] The comparative slower release of griseofulvin from MCM-

41-NH_2-GRIS could be attributed to the APTES grafting on the surface which may impart relatively slight hydrophobicity owing to the aminopropyl chain of APTES compared to MCM-41 leading to slower influx of dissolution media in the pore channels which would eventually delay the dissolution of griseofulvin. Also, APTES grafting would impart some steric hindrance inhibiting the release of griseofulvin from the pore channels.[50] Moreover, the positively charged amino groups may interact with negatively charged carbonyl groups, resulting in slower release from MCM-41-NH_2 compared to MCM-41. This finding is in accordance with an earlier report using emodin as the drug molecule.[51] Thus, the surface charge clearly demonstrates its role in modulating the drug release.

Hydrophobic modification of MCM-41 using methyl group results in poor influx of dissolution media in the pore channels leading to very slow dissolution of drug resulting in its slow release[27] which is also supported by the TGA curves in Figs. 6A and 7A. The presence of hydrophobic methyl groups reduces interaction of encapsulated griseofulvin with the aqueous media. On the other hand, the hydrophilic MCM-41 results in faster drug release of almost 2 order due to the easier influx of dissolution media in pore channels. Thus, hydrophobicity of MCM-41 materials controls the drug release can be attributed to the wetting effect with dissolution media. The enhanced release of griseofulvin from MCM-41-GRIS could be attributed to the presence of nano-sized aggregates of griseofulvin and absence of steric hindrance or hydrophobic moiety on its surface. The surface modified MSNs were prepared with similar pore size to avoid the pore size effect in drug release and solubility studies and it was found that, the surface charge and hydrophobicity plays a critical role in controlling griseofulvin's release from MSNs.

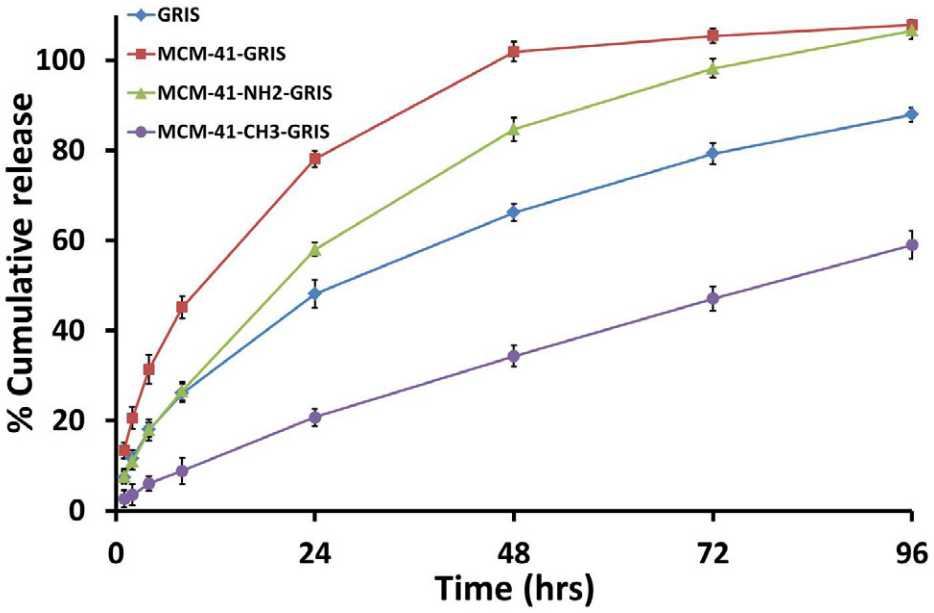

Fig 9. *In vitro* release of pure griseofulvin and griseofulvin loaded in MCM-41-GRIS, MCM-41-NH_2-GRIS and MCM-41-CH_3-GRIS materials in 0.5% SLS

The effect of *in vitro* release on MSNs particle size was studied by measuring their size using DLS. It was observed that the particle size of MSNs was slightly altered after *in vitro* release studies wherein particle size of MCM-41 (190 nm, PDI = 0.182), MCM-41-NH_2 (190 nm, PDI = 0.165) and MCM-41-CH_3 (190 nm, PDI = 0.223) changed to 190, 220 and 220 nm with PDI of 0.179, 0.198 and 0.232 respectively (Fig. 10).

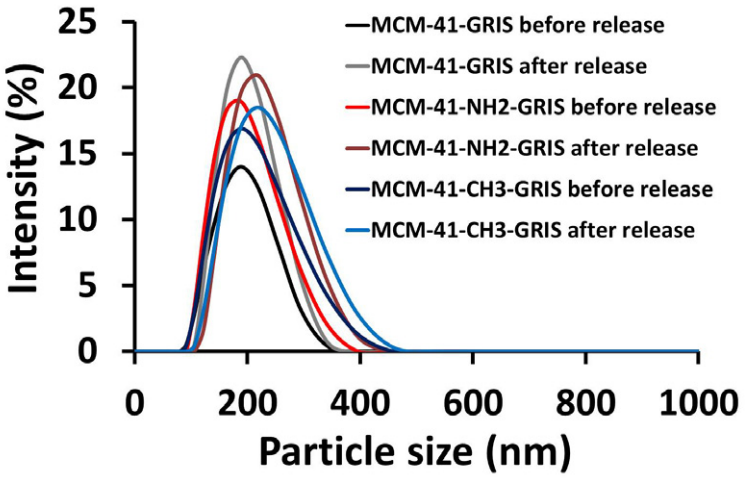

Fig. 10 Effect of *in vitro* dissolution on particle size of MCM-41-GRIS, MCM-41-NH_2-GRIS and MCM-41-CH_3-GRIS materials before and after release .

Griseofulvin solubility was determined by preparing saturated solution of GRIS, MCM-41-GRIS, MCM-41-NH_2-GRIS and MCM-41-CH_3-GRIS in water to reach equilibrium concentration. Griseofulvin solubility was increased approximately 3 folds in MCM-41-GRIS (62.3 µg ml^{-1}) compared to GRIS (21.5 µg ml^{-1}, Fig. 11) which is in accordance with previous studies using Indole-3-butyric acid and curcumin loaded in MCM-41.[18,20] . The enhanced solubility of griseofulvin in MCM-41-GRIS is attributed to its encapsulation in nanopores based on Ostwald-Freundlich equation where solubility enhancement is related to particle size.[7] The solubility was enhanced approximately 2 folds for MCM-41-NH_2-GRIS (39.8 µg ml^{-1}) compared to GRIS. The relatively low solubility of griseofulvin in MCM-41-NH_2-GRIS compared to MCM-41-GRIS could be attributed to the steric hindrance offered by the aminopropyl group grafted on its surface inhibiting the release of GRIS from the pore channels leading to comparatively decreased solubility.[50] However, the solubility of MCM-41-NH_2-GRIS is higher compared to pure GRIS as GRIS is a hydrophobic drug with low solubility and is present in crystalline state whereas for MCM-41-GRIS, MCM-41-NH_2-GRIS and MCM-41-CH_3-GRIS, GRIS is present in amorphous state as observed from Figs. 2B, 5 and 6B. Hydrophobic MCM-41-CH_3-GRIS (22.6 µg ml^{-1}) displayed solubility similar to that of pure griseofulvin due to the methyl groups present on its surface

leading to poor wetting of silica material and hence very slow influx of solvent in pore channels leading to low solubility. Thus, the surface functionalization in the form of surface charge and hydrophobicity leads to variation in the solubility profile of griseofulvin.

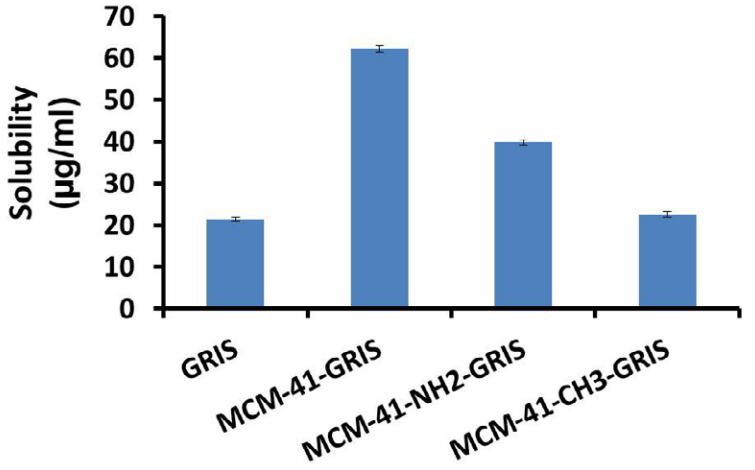

Fig 11. Saturated aqueous solubility of pure griseofulvin and griseofulvin encapsulated in MCM-41-GRIS, MCM-41-NH_2-GRIS and MCM-41-CH_3-GRIS samples.

4. Conclusion

MSNs were synthesized with different surface charge and hydrophobicity while retaining similar particle and pore size to study their influence on solubility and *in vitro* release of encapsulated griseofulvin. It was found that hydrophilic nanoparticles (MCM-41 and MCM-41-NH_2) enhanced the solubility and drug release compared to hydrophobic nanoparticles (MCM-41-CH_3) owing to their better wetting capability. Within hydrophilic nanoparticles, negatively charged particles (MCM-41) demonstrated 1.5 times higher solubility compared to positively charged nanoparticles (MCM-41-NH_2). Thus, both the solubility and release of griseofulvin can be modulated by carefully selecting the surface functionalization on MSNs. The findings from this study may provide new insight on rationally designed MSNs for applications in drug delivery.

Acknowledgement

We acknowledge the support from the Australian Research Council, the Australian National Fabrication Facility and the Australian Microscopy and Microanalysis Research Facility at the Centre for Microscopy and Microanalysis, The University of Queensland, Australia. We thank Ms Ying Yu from Centre of Microscopy and Microanalysis, The University of Queensland for SEM images.

References

(1) Lipinski, C. *Am. Pharm. Rev.* **2002**, *5*, 82-85. *Poor Aqueous Solubility – an Industry Wide Problem in Drug Discovery*.
(2) Nagarwal, R. C.*et. al. Curr. Drug Deliv.* **2011**, *8*, 398-406. *Nanocrystal Technology in the Delivery of Poorly Soluble Drugs: An Overview*.
(3) Gamsiz, E. D.*et. al. Ann. Biomed. Eng.* **2011**, *39*, 455-468. *Drug Salts and Solubilization: Modeling the Influence of Cyclodextrins on Oral Absorption*.
(4) Muela, S.*et. al. Int. J. Pharm.* **2010**, *384*, 93-99. *Influence of temperature on the solubilization of thiabendazole by combined action of solid dispersions and co-solvents*.
(5) Hsu, C.-M.*et. al. Carbohyd. Polym.* **2013**, *98*, 1422-1429. *Enhancement of rhubarb extract solubility and bioactivity by 2-hydroxypropyl-beta-cyclodextrin*.
(6) Pereira, J. M.*et. al. Mol. Pharamceut.* **2013**, *10*, 4640-4653. *Interplay of Degradation, Dissolution and Stabilization of Clarithromycin and Its Amorphous Solid Dispersions*.
(7) Ostwald, W. *Z Phys Che-Stoch Ve* **1900**, *34*, 495-503. *On the assumed isomerism of red and yellow mercury oxide and the surface-tension of solid bodies*.
(8) Couvreur, P.*et. al. Eur J Pharm Biopharm* **1995**, *41*, 2-13. *Controlled Drug-Delivery With Nanoparticles - Current Possibilities And Future-Trends*.
(9) Mulik, R. S.*et. al. Int. J. Pharm.* **2010**, *398*, 190-203. *Transferrin mediated solid lipid nanoparticles containing curcumin: Enhanced in vitro anticancer activity by induction of apoptosis*.
(10) Oussoren, C.*et. al. Adv Drug Deliver Rev* **2001**, *50*, 143-156. *Liposomes to target the lymphatics by subcutaneous administration*.
(11) Kresge, C. T.*et. al. Nature* **1992**, *359*, 710-712. *Ordered Mesoporous Molecular-Sieves Synthesized By A Liquid-Crystal Template Mechanism*.
(12) Zhao, D. Y.*et. al. J. Am. Chem. Soc.* **1998**, *120*, 6024-6036. *Nonionic triblock and star diblock copolymer and oligomeric surfactant syntheses of highly ordered, hydrothermally stable, mesoporous silica structures*.
(13) Szegedi, A.*et. al. J Solid State Chem.* **2011**, *184*, 1201-1207. *Effect of amine functionalization of spherical MCM-41 and SBA-15 on controlled drug release*.
(14) Vallet-Regi, M.*et. al. Chem. Mat.* **2001**, *13*, 308-311. *A new property of MCM-41: Drug delivery system*.
(15) He, J.*et. al. RSC Adv.* **2014**, *4*, 13304-13312. *Immobilization of papain on nanoporous silica*.
(16) Karimi, B.*et. al. RSC Adv.* **2014**, *4*, 4387-4394. *Immobilization, stability and enzymatic activity of albumin and trypsin adsorbed onto nanostructured mesoporous SBA-15 with compatible pore sizes*.
(17) Gu, J. L.*et. al. J. Colloid Interface Sci.* **2013**, *407*, 236-242. *Sub-150 nm mesoporous silica nanoparticles with tunable pore sizes and well-ordered mesostructure for protein encapsulation*.
(18) Jambhrunkar, S.*et. al. RSC Adv.* **2014**, *4*, 709-712. *Mesoporous silica nanoparticles enhance the cytotoxicity of curcumin*.
(19) Al-Obaidi, H.*et. al. AAPS Pharmscitech* **2009**, *10*, 1172-1177. *Evaluation of Griseofulvin Binary and Ternary Solid Dispersions with HPMCAS*.
(20) Ambrogi, V.*et. al. Micropor. Mesopor. Mat.* **2006**, *96*, 177-183. *Effect of MCM-41 on the dissolution rate of the poorly soluble plant growth regulator, the indole-3-butyric acid*.
(21) Jambhrunkar, S.*et. al. J. Am. Chem. Soc.* **2013**, *135*, 8444-8447. *Stepwise Pore Size Reduction of Ordered Nanoporous Silica Materials at Angstrom Precision*.
(22) Szegedi, A.*et. al. J Solid State Chem* **2012**, *194*, 257-263. *Controlled drug release on amine functionalized spherical MCM-41*.
(23) Lu, J.*et. al. Nanomedicine: NBM* **2012**, *8*, 212-220. *In vivo tumor suppression efficacy of mesoporous silica nanoparticles-based drug-delivery system: enhanced efficacy by folate modification*.
(24) Kamarudin, N. H. N.*et. al. Micropor. Mesopor. Mat.* **2013**, *180*, 235-241. *Role of 3-aminopropyltriethoxysilane in the preparation of mesoporous silica nanoparticles for ibuprofen delivery: Effect on physicochemical properties*.
(25) Xie, M.*et. al. Colloid Surface B* **2013**, *110*, 138-147. *A multifunctional mesoporous silica nanocomposite for targeted delivery, controlled release of doxorubicin and bioimaging*.
(26) Wani, A.*et. al. Pharm. Res.* **2012**, *29*, 2407-2418. *Surface Functionalization of Mesoporous Silica Nanoparticles Controls Loading and Release Behavior of Mitoxantrone*.

(27) Tang, Q. L.*et. al. J Control Release* **2006**, *114*, 41-46. *Studies on a new carrier of trimethylsilyl-modified mesoporous material for controlled drug delivery*.
(28) Aggarwal, N.*et. al. Int. J. Pharm.* **2012**, *437*, 277-287. *Preparation and evaluation of antifungal efficacy of griseofulvin loaded deformable membrane vesicles in optimized guinea pig model of Microsporum canis-Dermatophytosis*.
(29) Al-Obaidi, H.*et. al. Int. J. Pharm.* **2013**, *443*, 95-102. *Investigation of griseofulvin and hydroxypropylmethyl cellulose acetate succinate miscibility in ball milled solid dispersions*.
(30) Veiga, M. D.*et. al. J. Pharm. Sci.* **1998**, *87*, 891-900. *Interactions of griseofulvin with cyclodextrins in solid binary systems*.
(31) Aggarwal, N.*et. al. Colloid Surface B* **2013**, *105*, 158-166. *Formulation, characterization and evaluation of an optimized microemulsion formulation of griseofulvin for topical application*.
(32) Hbaieb, S.*et. al.* **2012**, *439*, 234-245. *Loading antifungal drugs onto silica particles grafted with cyclodextrins by means of inclusion complex formation at the solid surface*.
(33) Yang, S.*et. al. J. Am. Chem. Soc.* **2006**, *128*, 10460-10466. *On the origin of helical mesostructures*.
(34) Lu, J.*et. al. Small* **2007**, *3*, 1341-1346. *Mesoporous silica nanoparticles as a delivery system for hydrophobic anticancer drugs*.
(35) Kecht, J.*et. al. Chem. Mater.* **2008**, *20*, 7207-7214. *Selective Functionalization of the Outer and Inner Surfaces in Mesoporous Silica Nanoparticles*.
(36) Zhao, X. S.*et. al. J. Phys. Chem. B* **1998**, *102*, 1556-1561. *Modification of MCM-41 by surface silylation with trimethylchlorosilane and adsorption study*.
(37) Chen, Y.*et. al. Molecules* **2012**, *17*, 5972-5987. *Preparation of Curcumin-Loaded Liposomes and Evaluation of Their Skin Permeation and Pharmacodynamics*.
(38) Shao, J. F.*et. al. Acta Bioch. Bioph. Sin.* **2011**, *43*, 267-274. *Curcumin delivery by methoxy polyethylene glycol-poly(caprolactone) nanoparticles inhibits the growth of C6 glioma cells*.
(39) Yang, J.*et. al. J. Mater. Chem.* **2011**, *21*, 2489-2494. *A designed nanoporous material for phosphate removal with high efficiency*.
(40) Yang, C. M.*et. al. Chem. Mater.* **2003**, *15*, 275-280. *Highly dispersed metal nanoparticles in functionalized SBA-15*.
(41) Mello, M. R.*et. al. Microporous Mesoporous Mat.* **2011**, *143*, 174-179. *Amine-modified MCM-41 mesoporous silica for carbon dioxide capture*.
(42) Park, D. H.*et. al. Ind. Eng. Chem. Res.* **2001**, *40*, 6105-6110. *Enhancement of hydrothermal stability and hydrophobicity of a silica MCM-48 membrane by silylation*.
(43) Fang, Y.*et. al.* **2014**, *53*, 5366-5370. *Dual-Pore Mesoporous Carbon@ Silica Composite Core- Shell Nanospheres for Multidrug Delivery***.
(44) Pan, D. H.*et. al. J. Mater. Res.* **2011**, *26*, 804-814. *A silanol protection mechanism: Understanding the decomposition behavior of surfactants in mesostructured solids*.
(45) Nieto, A.*et. al. Micropor. Mesopor. Mat.* **2008**, *116*, 4-13. *Functionalization degree of SBA-15 as key factor to modulate sodium alendronate dosage*.
(46) Punyacharoennon, P.*et. al. J. Appl. Polym. Sci.* **2008**, *110*, 3336-3347. *Grafting and Phosphonic Acid Functionalization of Hyperbranched Polyamidoamine Polymer onto Ultrafine Silica*.
(47) Yang, J.*et. al. Vib. Spectrosc.* **2009**, *50*, 178-184. *Studies of the surface wettability and hydrothermal stability of methyl-modified silica films by FT-IR and Raman spectra*.
(48) Limnell, T.*et. al. J. Pharm. Sci.* **2011**, *100*, 3294-3306. *Drug Delivery Formulations of Ordered and Nonordered Mesoporous Silica: Comparison of Three Drug Loading Methods*.
(49) Vialpando, M.*et. al. J. Pharm. Sci.* **2011**, *100*, 3411-3420. *Evaluation of Ordered Mesoporous Silica as a Carrier for Poorly Soluble Drugs: Influence of Pressure on the Structure and Drug Release*.
(50) Jal, P. K.*et. al. Talanta* **2004**, *62*, 1005-1028. *Chemical modification of silica surface by immobilization of functional groups for extractive concentration of metal ions*.
(51) Xu, Y.*et. al. Appl. Surf. Sci.* **2012**, *258*, 6366-6372. *Improving the controlled release of water-insoluble emodin from amino-functionalized mesoporous silica*.

Graphical abstract:

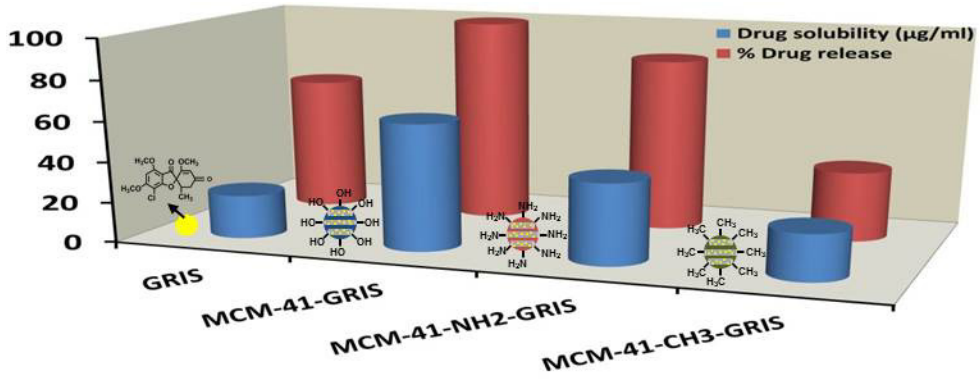

- The first example of controlled release of Griseofulvin using mesoporous materials
- A systematic study on the role of surface chemistry on solubility and drug release
- Hydrophilic silica particles enhanced solubility and drug release of Griseofulvin